Available online at www.sciencedirect.com
ScienceDirect
Mendeleev Commun., 2024, **34**, 737–739

Mendeleev Communications

Two-route formation of soot nuclei: experimental and modeling evidence

Emmanuel Busillo,[b] Pavel A. Vlasov,*[a,c] Vladimir N. Smirnov,[a]
Dmitrii I. Mikhailov[a] and Vladimir S. Arutyunov[a,b]

[a] *N. N. Semenov Federal Research Center for Chemical Physics, Russian Academy of Sciences, 119991 Moscow, Russian Federation. E-mail: shocktube@yandex.ru*
[b] *National University of Oil and Gas ‘Gubkin University’, 119991 Moscow, Russian Federation*
[c] *National Research Nuclear University MEPhI, 115409 Moscow, Russian Federation*

DOI: 10.1016/j.mencom.2024.09.036

The results of shock-tube measurements of acetylene concentration and characteristics of the ensemble of soot particles during the pyrolysis of benzene, ethylene, ethylene–methane and ethylene–propane diluted with argon are compared with the predictions of the unified kinetic model of soot formation implemented in the MACRON program based on the Galerkin method. The simulation results demonstrate good agreement with experimental data for the pyrolysis of ethylene alone and with the specified additives, thereby confirming the two-route mechanism of soot nuclei formation. The agreement for benzene pyrolysis is less satisfactory.

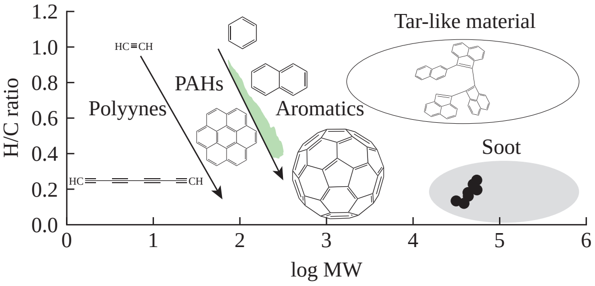

Keywords: ethylene, benzene, shock-tube experiments, soot nuclei formation, acetylene measurements, kinetic simulation.

Combustion-generated greenhouse gases and soot lead to air pollution and eventually to climate change,[1] a hazard that motivates improvements in combustion technologies, particularly as they relate to soot formation.[2–4] Acetylene (C_2H_2) has been shown to play a key role in the growth of soot particles *via* the HACA (H-Abstraction–Acetylene-Addition) mechanism,[5] although little is known about how it participates in the formation of soot nuclei. Parameters such as soot induction period (τ), soot volume fraction (f_v), soot yield (SY), average particle size and/or soot concentration are commonly measured, while concentrations of important gaseous species such as C_2H_2 are rarely measured in parallel. The only exception known to us is a study[6] in which time-resolved acetylene concentration and SY value were measured concurrently behind reflected shock waves at 1600–2200 K and 3–5 bar. These measurements prompted us to carry out experiments on the pyrolysis of benzene (C_6H_6) and ethylene (C_2H_4) in argon bath gas behind reflected shock waves and to perform detailed kinetic simulations of our own and published[6,8,9] experimental data using the reaction mechanism from the cited work[10] in conjunction with the MACRON solver based on the Galerkin method.[11]

Details of the experimental procedure and data processing can be found elsewhere.[6,10,12,13] Note that in typical shock-tube experiments the observation period is limited to ~1.5–2.0 ms, which imposes restrictions on studying later stages of soot formation.[7] Another important point is that in our experiments, at a benzene concentration of more than 1%, the probing radiation was almost

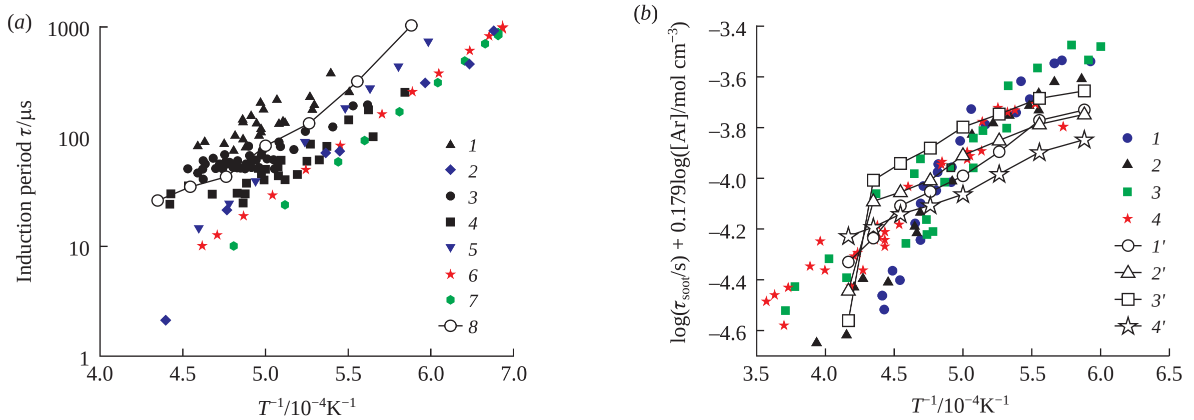

Figure 1 Temperature dependences of the induction time of soot formation during the pyrolysis of various hydrocarbon–Ar mixtures. (*a*) Values for benzene obtained experimentally using (*1*) 0.5% C_6H_6,[8] (*2*) 1% C_6H_6,[6] (*3*) 1% C_6H_6[8] and (*4*) 2% C_6H_6,[8] as well as in the works of (*5*) Kellerer *et al.*,[9] (*6*) Tanke[15] and (*7*) Koch *et al.*,[9] and by simulation for (*8*) 1% C_6H_6 in this work. (*b*) Values for acetylene obtained experimentally[16] for (*1*) 4.65% C_2H_2 (p = 2 bar), (*2*) 4.65% C_2H_2 (p = 0.8 bar), (*3*) 1.09% C_2H_2 (p = 3 bar) and (*4*) 20.0% C_2H_2 (p = 0.3 bar), and also by simulation for (*1′*) 4.65% C_2H_2 (p = 2.3 bar), (*2′*) 4.65% C_2H_2 (p = 1.0 bar), (*3′*) 1.09% C_2H_2 (p = 3 bar) and (*4′*) 20.0% C_2H_2 (p = 0.3 bar) in this work.

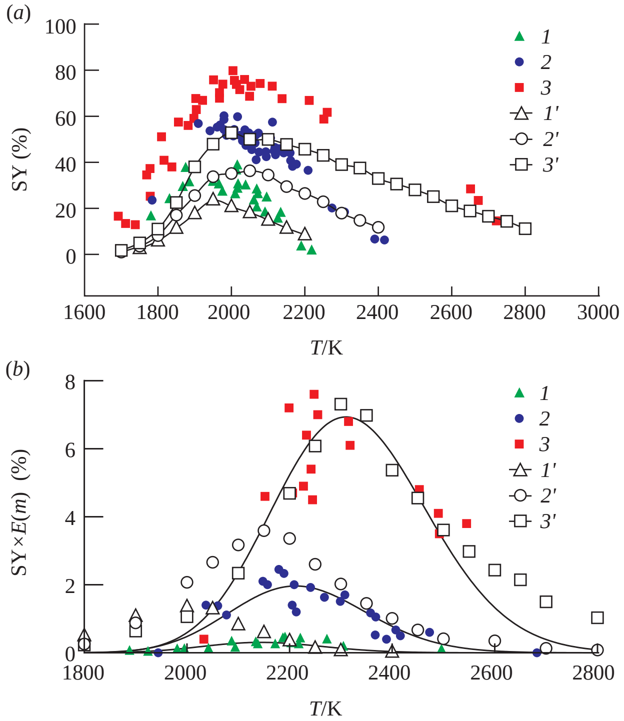

Figure 2 Temperature dependences of SY during the pyrolysis of hydrocarbon–Ar mixtures (*a*) at an initial benzene concentration of (*1*),(*1′*) 0.5%, (*2*),(*2′*) 1% and (*3*),(*3′*) 2%, as well as (*b*) at an initial ethylene concentration of (*1*),(*1′*) 1.5%, (*2*),(*2′*) 3.0% and (*3*),(*3′*) 5.0%, with given parameters $E(m) = 0.37$ and $\tau_r = 1.5$ ms. The data were obtained (*1*)–(*3*) experimentally[8] and (*1′*)–(*3′*) calculated in this work. The lines represent the log-normal approximation of the results of our calculations.

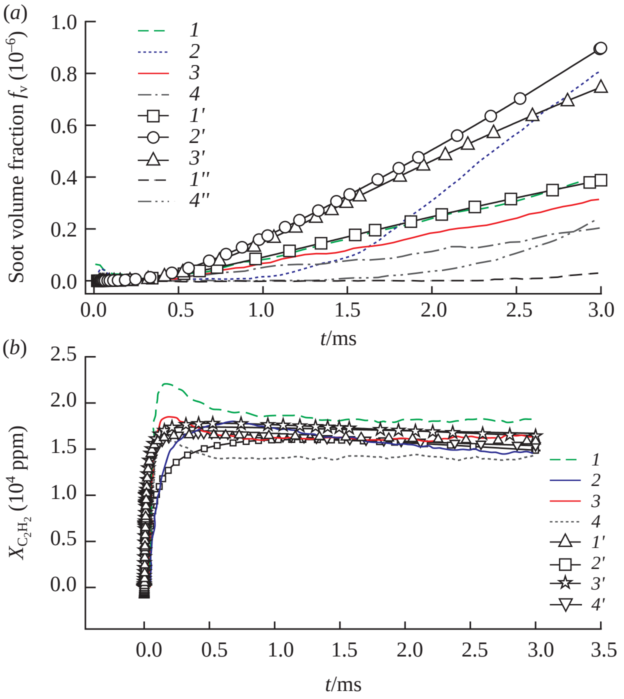

Figure 3 Time dependences of (*a*) the soot volume fraction and (*b*) the mole fraction of acetylene ($X_{C_2H_2}$) behind reflected shock waves during the pyrolysis of C_2H_4–Ar mixtures with and without CH_4 and C_3H_8 additives: (*1*),(*1′*),(*1″*) C_2H_4 ($T_{50} = 2179$ K), (*2*),(*2′*) $C_2H_4 + CH_4$ ($T_{50} = 1961$ K), (*3*),(*3′*) $C_2H_4 + C_3H_8$ ($T_{50} = 2132$ K) and (*4*),(*4′*),(*4″*) $C_2H_4 + CH_4$ ($T_{50} = 2136$ K). T_{50} is the temperature immediately after the front of the reflected shock wave. The data were obtained (*1*)–(*4*) experimentally[6] and calculated (*1′*)–(*4′*) in this work or (*1″*),(*4″*) in the cited works.[6,10]

completely absorbed, which did not make it possible to determine the volume fraction of soot.

The measured and simulated soot induction times for the pyrolysis of different mixtures of benzene and acetylene in argon are shown in Figure 1(*a*),(*b*).

As can be seen, the simulations we performed using the unified kinetic model of soot formation[10] closely reproduce the induction periods measured in this work and other studies.

Figure 2(*a*),(*b*) demonstrates good agreement between measured and simulated SY values. As can be seen, there is an evident dependence of SY on the initial concentration of hydrocarbons. When comparing the simulation results with the experimental data, we assumed that the optical properties of soot are the same for all hydrocarbons, characterized by a constant value of the absorption function $E(m) = 0.37$.[10,12,13] The refractive index absorption function for a particular wavelength $E(m)$ can be represented as

$$E(m) = -\,\mathrm{Im}\left(\frac{m^2-1}{m^2+2}\right) = \frac{6kn}{(n^2-k^2+2)^2+4k^2n^2},$$

where $m = n - ik$ is the complex refractive index of soot, and i is the imaginary unit. The details of the experiment are presented in Online Supplementary Materials.

As can be seen in Figure 2(*a*),(*b*), with increasing hydrocarbon concentration, the SY maximum shifts towards higher temperatures, which can be explained by a greater decrease in temperature caused by hydrocarbon pyrolysis. In the case of benzene, it should be noted that due to almost complete absorption of probing radiation (see above), the results obtained[8] for a 2% C_6H_6 mixture should be treated with caution.

Comparison of the simulated and experimental results for C_2H_4 pyrolysis with and without additives [Figure 3(*a*),(*b*)] led us to several important conclusions. It is quite clear that the calculations based on the kinetic mechanism proposed in the cited work[6] deviate from their own experimental measurements by more than an order of magnitude [Figure 3(*a*), curves *1* and *1″*]. At the same time, our calculations almost completely reproduce the experimental data[6] both on the soot volume fraction f_v [Figure 3(*a*), curves *1* and *1′*] and on the C_2H_2 concentration [Figure 3(*b*)]. For the ethylene–methane mixture, the agreement between the experimental and theoretical results[6] is substantially better [Figure 3(*a*), curves *4* and *4″*]; our simulations also correctly, but not perfectly, describe these results [Figure 3(*a*), curves *1*–*3* and *1′*–*3′*].

Our model also reasonably well reproduces the time dependence of f_v for the C_2H_4–C_3H_8 mixtures. As can be seen from Figure 3(*b*), for all three cases, with and without additives, the time profiles of the C_2H_2 concentration vary insignificantly, suggesting that the behavior of the acetylene concentration cannot be the reason for such a large discrepancy between the soot volume fractions calculated using the unified kinetic model and the kinetic model in the cited work.[6] In our opinion, the main difference between these models lies in the postulated process of soot inception. The authors of that work[6] assumed, in fact, that soot nuclei are formed from sufficiently large fragments of aromatic and polyaromatic hydrocarbons containing from 36 to 48 carbon atoms. However, the formation of such large polyaromatic fragments takes a long time, sufficiently exceeding that achievable in shock-tube experiments. Along with the aromatic route of soot inception, which implicates relatively small fragments containing two to three six- and five-membered rings, our unified kinetic model includes another pathway involving aliphatic fragments (C_8H_4) with alternating single, double and triple bonds. In ethylene pyrolysis, the second pathway dominates, and therefore, its inclusion ensures better agreement between the measured and calculated time profiles of the soot volume fraction. The addition of CH_4 or C_3H_8 to C_2H_4–Ar mixtures leads to the formation of radicals with an odd number of carbon atoms, which is a factor that enhances the role of the polyaromatic route for soot inception. Small additions of oxygen have also been shown to stimulate soot formation during acetylene pyrolysis for the same reason.[17]

Thus, comparison of the measured characteristics of soot formation with the predictions of our unified kinetic model of soot formation in the pyrolysis of C_2H_2, C_2H_4 and C_6H_6 diluted with argon led us to the conclusion that both routes contribute to the formation of soot nuclei, but differently for different hydrocarbons. In the case of benzene pyrolysis, the polyaromatic pathway for the formation of soot particle nuclei is dominant. For the pyrolysis of acetylene and ethylene, the polyynic pathway is more important. The addition of methane or propane to ethylene–argon mixtures boosts the polyaromatic nucleation pathway, thereby increasing soot yield.

Online Supplementary Materials

Supplementary data associated with this article can be found in the online version at doi: 10.1016/j.mencom.2024.09.036.

References

1 K. Handayani, T. Filatova, Y. Krozer and P. Anugrah, *Appl. Energy*, 2020, **262**, 114485; https://doi.org/10.1016/j.apenergy.2019.114485.

2 A. Gharehghani, K. Ghasemi, M. Siavashi and S. Mehranfar, *Fuel*, 2021, **304**, 121411; https://doi.org/10.1016/j.fuel.2021.121411.

3 K. Kohse-Höinghaus, *Proc. Combust. Inst.*, 2021, **38**, 1; https://doi.org/10.1016/j.proci.2020.06.375.

4 Y. Ju, C. B. Reuter, O. R. Yehia, T. I. Farouk and S. H. Won, *Prog. Energy Combust. Sci.*, 2019, **75**, 100787; https://doi.org/10.1016/j.pecs.2019.100787.

5 M. Frenklach and A. M. Mebel, *Phys. Chem. Chem. Phys.*, 2020, **22**, 5314; https://doi.org/10.1039/d0cp00116c.

6 K. C. Utsav, M. Beshir and A. Farooq, *Proc. Combust. Inst.*, 2017, **36**, 833; https://doi.org/10.1016/j.proci.2016.08.087.

7 A. V. Eremin, *Prog. Energy Combust. Sci.*, 2012, **38**, 1; https://doi.org/10.1016/j.pecs.2011.09.002.

8 R. Starke and P. Roth, *Combust. Flame*, 2002, **127**, 2278; https://doi.org/10.1016/S0010-2180(01)00329-7.

9 H. Kellerer, A. Müller, H.-J. Bauer and S. Wittig, *Combust. Sci. Technol.*, 1996, **113**, 67; https://doi.org/10.1080/00102209608935488.

10 G. L. Agafonov, I. V. Bilera, P. A. Vlasov, I. V. Zhil'tsova, Yu. A. Kolbanovskii, V. N. Smirnov and A. M. Tereza, *Kinet. Catal.*, 2016, **57**, 557; https://doi.org/10.1134/S0023158416050013.

11 J. Ackermann and M. Wulkow, *Konrad-Zuse-Zentrum für Informationstechnik Berlin, Preprint SC 90-14*, 1990; https://nbn-resolving.org/urn:nbn:de:0297-zib-423.

12 G. L. Agafonov, P. A. Vlasov and V. N. Smirnov, *Kinet. Catal.*, 2011, **52**, 358; https://doi.org/10.1134/s0023158411030013.

13 G. L. Agafonov, I. V. Bilera, P. A. Vlasov, Yu. A. Kolbanovskii, V. N. Smirnov and A. M. Tereza, *Kinet. Catal.*, 2015, **56**, 12; https://doi.org/10.1134/S0023158415010012.

14 H. Kellerer, R. Koch and S. Wittig, *Combust. Flame*, 2000, **120**, 188; https://doi.org/10.1016/S0010-2180(99)00067-X.

15 D. Tanke, *PhD Thesis*, Georg August University of Göttingen, Göttingen, 1994; https://doi.org/10.53846/goediss-5086.

16 M. Frenklach, S. Taki, M. B. Durgaprasad and R. A. Matula, *Combust. Flame*, 1983, **54**, 81; https://doi.org/10.1016/0010-2180(83)90024-X.

17 E. Busillo, P. Vlasov and V. Arutyunov, *Mendeleev Commun.*, 2022, **32**, 700; https://doi.org/10.1016/j.mencom.2022.09.045.

Received: 11th April 2024; Com. 24/7459